

ELECTROMAGNETIC STEADY MOTION OF CASSON FLUID WITH HEAT AND MASS TRANSFER THROUGH POROUS MEDIUM PAST A SHRINKING SURFACE

by

**Nabil T. ELDABE^a, Mohamed Y. ABOU-ZEID^a, Omar H. EL-KALAAWY^b,
Salah M. MOAWAD^b, and Ola S. AHMED^{b*}**

^a Department of Mathematics, Faculty of Education, Ain Shams University,
Roxy, Cairo, Egypt

^b Department of Mathematics and Computer Science, Faculty of Science,
Beni-Suef University, Egypt

Original scientific paper

<https://doi.org/10.2298/TSCI190418416E>

The motion of non-Newtonian fluid with heat and mass transfer through porous medium past a shrinking plate is discussed. The fluid obeys Casson model, heat generation, viscous dissipation, thermal diffusion, and chemical reaction are taken in our considered. The motion is modulated mathematically by a system of non-linear PDE which describe the continuity, momentum, heat, and mass equations. These system of non-linear equations are transformed into ODE by using a suitable transformations. These equations are solved numerically by using MATHEMATICA package. The numerical distributions of the velocity, temperature, and concentration are obtained as a functions of the physical parameters of the problem. Moreover, the effects of these parameters on these solutions are discussed numerically and illustrated graphically through some figures. It is clear that these parameters play an important role to control the velocity, temperature, and concentration of the fluid motion. It is found that the fluid velocity decreases with the increasing of electric parameter while it increases as the magnetic Hartman parameter increases, these results is good agreement with the physical situation. Also, the fluid temperature decreases and increases as the Prandtl number and Eckert number increases, respectively. At least the fluid concentration decreases with both of Soret and Schmidt numbers.

Key words: *electromagnetichydrodynamic, Casson fluid, heat and mass transfer, porous medium*

Introduction

The study of non-Newtonian fluid has gained a big importance due to it's applications such as in industry and engineering. Due to the sub-stances contained like fibrinogen, protein and the blood Cell's chain structure, the human blood can be classified as Casson fluid. Pramanik [1] investigated the properties of heat transfer of Casson fluid through thermal radiation and porous medium. The effects of second order slip in a channel on plane Poiseuille nanofluid through the influence of Stefan are discovered by Ellahi *et al.* [2]. Akbar [3] investigated the exact solution of magnetic field effect in an asymmetric channel on peristaltic flow of a Casson fluid. Ellahi *et al.* [4] investigated the 2-D mixed heat transfer and convection flow

* Corresponding author, e-mail: master_math2003@yahoo.com

in ferromagnetic fluid past a stretching sheet. Analysis of non-Newtonian fluid and heat transfer through an oscillating vertical plate on an unsteady boundary-layer of a Casson fluid is studied by Hussanan *et al.* [5]. Abou-Zeid [6] studied the motion of incompressible micropolar non-Newtonian nanofluid with heat transfer in asymmetric channel. The unsteady peristaltic mechanism with heat and mass transfer of an incompressible micropolar non-Newtonian fluid in 2-D channel is discussed by El-Dabe and Abou-Zeid [7]. Water base nanofluid flow in a porous medium over wavy surface is investigated by Hassan *et al.* [8]. Abou-Zeid [9] investigated the MHD non-Newtonian nanofluid flow through a porous medium in eccentric annuli with peristalsis. Jeffery nanofluid peristaltic flow through a vertical tube is studied by El-Dabe *et al.* [10].

Heat and mass transfer are kinetic processes that may occur and be studied separately or jointly. Studying them a part is simpler, but both processes are modeled by similar mathematical equations in the case of diffusion and convection. Besides heat and mass transfer must be jointly considered in some cases like evaporative cooling and ablation. Combined mass and heat transfer problems have an important in many processes and it is notable in recent years such as evaporation on a water surface, drying, process of the connection with thermal recovery, chemical industry. Mass and heat transfer occurs at the same time, for example in the power industry, it's a way of generating energy in which the energy is extracted directly from a moving fluid. There are wide industrial applications of melting heat transfer such as welding and magma solidification, casting, thawing of frozen ground and perma-frost melting. Kataria and Patel [11] investigated heat and mass transfer characteristics in the unsteady MHD Casson fluid flow past over an oscillating vertical plate. The effects of heat and mass transfer on MHD Eyring-Powell fluid under long-wavelength approximation and low Reynolds is investigated by Shaaaban and Abou-Zeid [12]. Ellahi *et al.* [13] discussed mixed heat transfer and convection boundary-layer flow past a vertical slender cylinder. Raju *et al.* [14] discussed the heat and mass transfer behavior of Casson fluid past an exponentially permeable stretching surface in presence of thermal radiation. Shehzad *et al.* [15] investigated the effect of mass transfer in MHD flow of a Casson fluid over a porous stretching sheet. The motion of non-Newtonian nanofluid over a stretching sheet through a non-Darcy porous medium with heat and mass transfer is studied by El-Dabe *et al.* [16].

The MHD represent an interdisciplinary science such as electro-chemistry, electro-statics, thermo-physics, and hydro-dynamics. Electrode configuration plays an important role to find the efficiency of the electrohydrodynamic (EHD) process. Alamir *et al.* [17] studied the effects of mass transfer on MHD subjected to the heat transfer towards stretching cylinder. The MHD thermal boundary-layer of Cu-water nanofluids past an exponentially permeable stretching plate is discussed by Yousif *et al.* [18]. Hassan *et al.* [19] investigated convective mass and heat transfer of nanofluid through non-magnetic and magnetic nanomaterials under the magnetic influence. Chirkov *et al.* [20] studied the effect of liquid conductivity on the efficiency of EHD heat exchanger with charge formed by injection. The EHD flows and heat transfer in the blade-plane electrode system is investigated by Kuzko [21]. The heat transfer effects on MHD boundary-layer flow over non-isothermal stretching sheet is discussed by Abou-Zeid [22]. The heat characteristic with the non-darcian is studied by Pal and Mondal [23] under the effect of ohmic dissipation and thermal radiation.

The main aim of this work is to extend the work of Pal and Mondal [23] in the case of non-Newtonian fluid motion with heat and mass transfer, and include the viscous dissipation, heat generation, thermal diffusion, and chemical reaction effects. Then the boundary-layer motion of Casson incompressible, conducting fluid with heat and mass transfer over a horizontal

plate is investigated. The system is stressed by a uniform magnetic field and uniform electric field. A heat generation with radiation and chemical reaction are taken in consideration. This motion is modulated mathematically by a system of non-linear PDE which transformed into non-linear ODE by using suitable transformation. This system is solved numerically subjected to the appropriate boundary conditions to obtain the velocity, temperature, and concentration fields. The influences of the physical parameters of the problem on these solutions are discussed numerically and illustrated graphically through a set of figures. The ready analysis can render as a model which may support in comprehension the mechanics of physiological flows. Physically, our model corresponds to the transmission of the gastric juice in the small intestine.

Mathematical formulations

Consider a non-Newtonian electrically conducting incompressible fluid flowing over a shrinking sheet under the magnetic and electric fields as shown in fig. 1. Choose Cartesian co-ordinates (x, y, z) , where x is along the sheet, y is perpendicular to it, and z is normal to x - y plane. We know from Ohm law that $J = \sigma(E + V \times B)$ and Maxwell equations $\nabla B = 0$ and $\nabla \times E = 0$. The external applied magnetic field $B = (0, B_0, 0)$ while the electric field $E = (0, 0, -E_0)$.

The rheological of state for an incompressible and iso-tropic flow of a Casson fluid is as follows [24]:

$$\tau_{ij} = \begin{cases} 2 \left(\mu_B + \frac{p_y}{\sqrt{2\pi}} \right) e_{ij}, & \pi > \pi_c \\ 2 \left(\mu_B + \frac{p_y}{\sqrt{2\pi_c}} \right) e_{ij}, & \pi < \pi_c \end{cases}$$

where π is the product of the component of deformation rate $\pi = e_{ij}e_{ij}$, π_c – a critical value of this product based on non-Newtonian model, μ_B – the plastic dynamic viscosity of the non-Newtonian fluid, and p_y – the yield stress of the fluid.

The governing boundary-layer equations for momentum, temperature, concentration equations can be written as [23]:

Continuity equation

$$\frac{\partial u}{\partial x} + \frac{\partial v}{\partial y} = 0 \tag{1}$$

Momentum equation

$$u \frac{\partial u}{\partial x} + v \frac{\partial u}{\partial y} = \nu \left(1 + \frac{1}{\beta} \right) \frac{\partial^2 u}{\partial y^2} + \frac{\sigma}{\rho} (E_0 B_0 - B_0^2 u) - \frac{\nu}{k} u \tag{2}$$

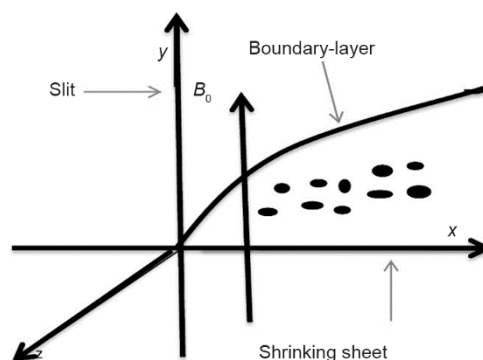


Figure 1. Boundary-layer over shrinking sheet

where u and v are the velocity components in the x - and y -directions, ν – the kinematic viscosity, ρ – the density, and k – the permeability of the porous medium. The boundary conditions on the velocity are appear under the effect of shrinking surface causing in x -direction:

$$\begin{aligned} u = U(x) = -bx & \quad v = 0 \quad \text{at} \quad y = 0 \\ u = 0 & \quad \text{as} \quad y \rightarrow \infty \end{aligned} \quad (3)$$

By using the following transformations:

$$u = -bx f'(\eta), \quad v = \sqrt{bv} f(\eta), \quad \eta = \sqrt{\frac{b}{\nu}} y \quad (4)$$

where $f(\eta)$ is the dimensionless stream function, and η – the similarity variable. Substitution of eq. (3) in eq. (2) we get:

$$\left(1 + \frac{1}{\beta}\right) f''' = f'^2 + ff'' + \text{Ha}^2 (E_1 - f') + K_1 f' \quad (5)$$

It is clear that the eq. (5) is third-order non-linear ODE for Casson fluid, if $\beta \rightarrow \infty$ the fluid becomes ordinary Newtonian, where $K_1 = (vbx)/k$ is the porous parameter, $\text{Ha}^2 = (\sigma B_0^2)/\rho b$ – the Hartman number, and $E_1 = E_0/(B_0 bx)$ – the local electric parameter. The boundary conditions in the non-dimensional form are:

$$f(0) = 0, \quad f'(0) = 1, \quad f'(\infty) = 0 \quad (6)$$

Heat transfer equation

The equation of heat transfer with thermal radiation, heat generation, ohmic dissipation, and viscous dissipation is given by:

$$u \frac{\partial T}{\partial x} + v \frac{\partial T}{\partial y} = \frac{k}{\rho c_p} \frac{\partial^2 T}{\partial y^2} + \frac{\mu}{\rho c_p} \left(1 + \frac{1}{\beta}\right) \left(\frac{\partial u}{\partial y}\right)^2 + \frac{\sigma}{\rho c_p} (uB_0 - E_0)^2 - \frac{1}{\rho c_p} \frac{\partial q_r}{\partial y} + G(T - T_\infty) \quad (7)$$

where c_p is specific heat at constant pressure, and k – the thermal conductivity. The boundary conditions on the temperature can be written:

$$T = T_\infty \quad \text{as} \quad y \rightarrow \infty \quad (8)$$

$$T = T_w \quad \text{as} \quad y = 0 \quad (9)$$

where T_w stands for shrinking sheet temperature, and T_∞ – the temperature far away from the shrinking sheet. The thermal radiation heat flux, q_r , is given by:

$$q_r = -\frac{4\sigma^*}{3k_0} \frac{\partial T^4}{\partial y} \quad (10)$$

where k_0 is the mean absorption coefficient, and σ^* – the Stefan-Boltzmann constant. We assume that the fluid-phase temperature differences in the flow are sufficient small such that T^4 may be expressed as a linear function of temperature:

$$T^4 = 4T_\infty^3 T - 3T_\infty^4 \quad (11)$$

We assume that dimensionless temperature variable $\theta(\eta)$ in the form:

$$\theta = \frac{T - T_\infty}{T_w - T_\infty} \quad (12)$$

By substitution of eqs. (10)-(12) in eq. (7) we get the non-dimensional thermal boundary-layer equation:

$$\frac{1 + N_r}{Pr} \theta'' = -f\theta' + EcHa^2 (f' + E_1)^2 - \left(1 + \frac{1}{\beta}\right) EcF''^2 - G\theta \quad (13)$$

where Pr is Prandtl number $[= (\rho\nu c_p)/k]$, N_r – the thermal radiation parameter $[= (16\sigma^* T_\infty^3)/3k^2]$, and Ec – the Eckert number $[=(b^2 x^2)/(c_p \Delta T)]$. The boundary condition of eqs. (8) and (9) becomes:

$$\theta(0) = 1 \quad \theta(\infty) = 0 \quad (14)$$

Concentration equation

The equation of concentration with thermal diffusion is given by:

$$u \frac{\partial c}{\partial x} + v \frac{\partial c}{\partial y} = D_m \frac{\partial^2 c}{\partial y^2} - A(c - c_\infty) + \frac{Dk_t}{T_w} \frac{\partial^2 T}{\partial y^2} \quad (15)$$

where D_m is the coefficient of mass diffusivity, k_t – the thermal diffusion ratio, and A – the reaction rate constant. The appropriate boundary conditions on the concentration are:

$$C = C_\infty \quad \text{as } y \rightarrow \infty \quad (16)$$

$$C = C_w \quad \text{as } y = 0 \quad (17)$$

Introduce the following quantity:

$$\phi = \frac{C - C_\infty}{C_w - C_\infty} \quad (18)$$

By substitution eq. (18) into eq. (15) we obtain non-dimensional thermal boundary-layer equation:

$$\frac{1}{Sc} \phi'' = f\phi' + \delta\phi - Sr\theta'' \quad (19)$$

where Sc is the Schmidt number $(= \nu/\alpha)$, δ – the chemical reaction $[= (AT_w)/(D_mk_t)]$, Sr – the Soret number $[= (D_mk_t)/(\nu\Delta C)]$. The boundary conditions become:

$$\phi(0) = 1 \quad \phi(\infty) = 0 \quad (20)$$

Numerical solutions

The system of eqs. (5), (13), and (19) are highly non-linear ODE. So, let $f = Y_1$, $\theta = Y_4$, and $\phi = Y_6$.

Hence, eqs. (5), (13), and (19) can be written:

$$\begin{aligned}
 Y_1' &= Y_2, & Y_2' &= Y_3, & Y_3' &= \frac{1}{1+\beta^{-1}} [Y_1^2 + Y_1 Y_3 + \text{Ha}^2 (E_1 - Y_2) + K_1 Y_2] \\
 Y_4' &= Y_5, & Y_5' &= \frac{\text{Pr}}{1+N_r} [-Y_1 Y_5 + \text{Ec Ha}^2 (Y_2 + E_1)^2 - (1+\beta^{-1}) \text{Ec} Y_3^2 - G\theta] \\
 Y_6' &= Y_7, & Y_7' &= Y_1 Y_7 + \delta Y_6 - \text{Sr} Y_5'
 \end{aligned} \quad (21)$$

where prime denotes to differentiation with respect to η and this system of eqs. (21) subject to the boundary conditions:

$$\begin{aligned}
 Y_1 &= 0, & Y_2 &= 0, & Y_4 &= 1, & Y_6 &= 1, & \text{at } \eta &= 0 \\
 Y_2 &= 0, & Y_4 &= 0, & Y_6 &= 0, & \text{at } \eta &\rightarrow \infty
 \end{aligned} \quad (22)$$

To apply shooting technique we use NAG FORTRAN library, namely, the subroutine D02HAF which requires the guessing of starting values of missing initial and terminal conditions. Rung-Kutta-Merson method with variable step size is used in this subroutine in order to control the local truncation error, then modified Newton-Raphson technique is applied to make successive corrections to the estimated boundary values. The process is repeated iteratively until convergence is obtained *i. e.* until the absolute values of the difference between every two successive approximations of the missing conditions is less than ε (in our case ε is taken = 10^{-6}).

Discussion

Figures 2 and 3 display the change of the velocity *vs.* the dimensionless co-ordinate, η , for several values of Hartmann number, and the electric field parameter, E_1 , respectively. It is seen, from these figures that the velocity increases with the increase of Hartmann number, this due to the fact that the effect of the magnetic field on electrically conductive fluid creates a drag force and develops the force known as Lorentz force which reduces the fluid motion, whereas it decreases as E_1 increases. For small values of E_1 , and large values of Hartmann number, the relation between f' and η is approximately a straight line. The behavior of f' for various values of K_1 is exactly similar to the behavior of f' for various values of Hartmann number given in fig. 2. The results which are obtained in fig. 2, are in agreement with those which are presented by Abou-Zeid *et al.* [25, 26].

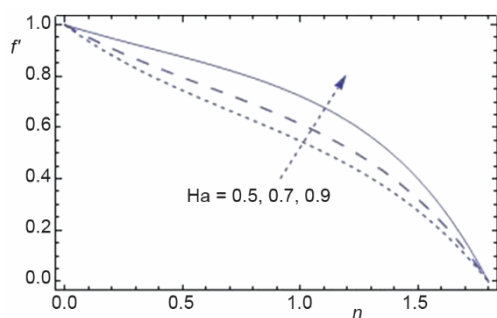


Figure 2. The velocity component is plotted against η for the variation value of Ha

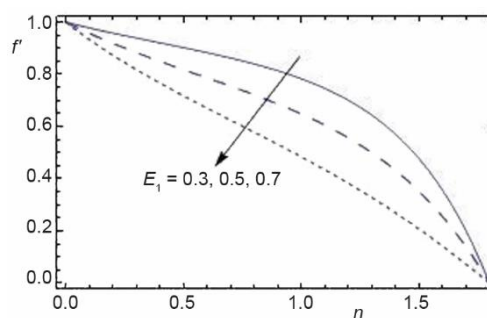


Figure 3. The velocity component is plotted against η for the variation value of E_1

Figures 4 and 5 represent the behaviors of the temperature distribution, θ , with the dimensionless co-ordinate, η , for different values of Eckert number and Prandtl number, respectively. It is observed from fig. 4 that the temperature distribution increases with the increase of Eckert number. The results which are obtained in fig. 4, are in agreement with those which are presented by El-Dabe *et al.* [10], and in fig. 5 the temperature decreases as Prandtl number increases. The thermal boundary-layer thickness may be reduced by increasing Prandtl number.

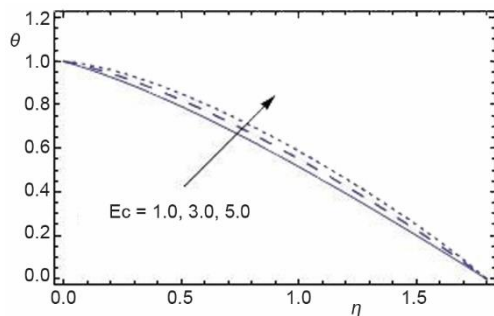


Figure 4. The temperature component is plotted against η for the variation value of Ec

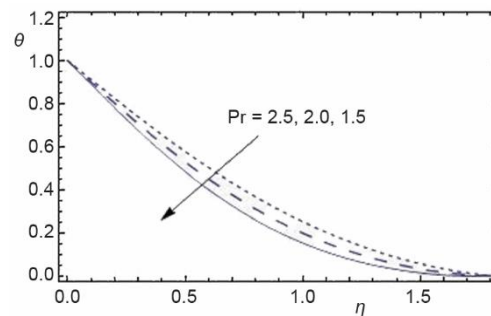


Figure 5. The temperature component is plotted against η for the variation value of Pr

In heat transfer problems, the Prandtl number rule the comparative thickening of the momentum and thermal boundary-layer. It is also noted that the difference of the temperature distribution for different values of Prandtl number becomes, and for large values of Prandtl number the relation between θ and η is approximately linear. The results which are obtained in fig. 5, are in agreement with those which are presented by Pramanik [1]. Moreover, While, for different values of Eckert number the relation between θ and η is a parabolic, *i. e.* as η increases, θ increases till a maximum value after which it decreases. The following explains the result in fig. 4, the effect of the source and dissipation temperature is to increase the rate of energy transport to the fluid and, accordingly, the temperature of the fluid.

Figures 6 and 7 show the behavior of the concentration, ϕ , with the dimensionless co-ordinate, η , for various values of Schmidt and Soret numbers, respectively. It has been noticed that the concentration increases with the decreases of both Schmidt and Soret numbers. It is also noted that for each value of both Schmidt and Soret numbers, there exists a minimum value of ϕ which increases by increasing both Schmidt and Soret numbers, and all minimum values occur at $\eta \cong 1.2$. The result in fig. 6 is due to the increase of Schmidt number is means a decreases of molecule diffusion. Hence, the concentration of the space is lower for small values

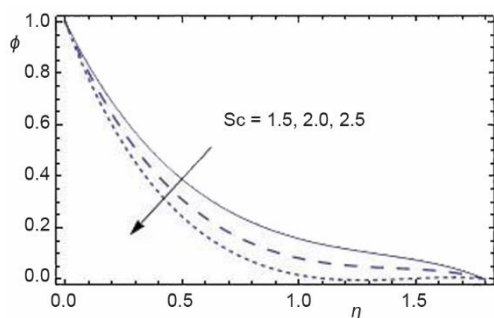


Figure 6. The concentration component is plotted against η for the variation value of Sc

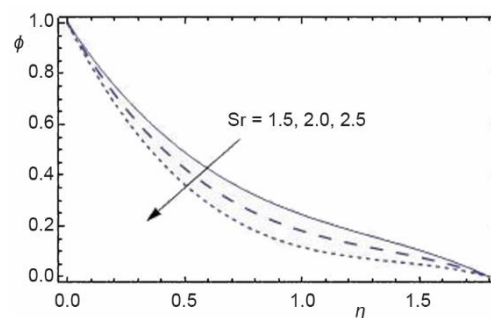


Figure 7. The concentration component is plotted against η for the variation value of Sr

of Schmidt number and higher for large values of Schmidt number. The results which are obtained in fig. 6, are in agreement with those which are presented by Kataria and Patel [11].

Table 1 presents a comparison between the numerical results of present study and those obtained by Pal and Mondal [23] for Nusselt number $-\theta'(0)$ for various values of both Prandtl and Hartmann numbers. It can be concluded from tab. 1 that the present results are in a good agreement with those obtained by Pal and Mondal [23].

Table 1. Verification of the model

Pr	Ha	$-\theta'(0)$ in the present work	$-\theta'(0)$ in the work of Pal and Mondal [23]
1	1	1.19268	1.33333
2	1	1.94141	1.99999
3	1	2.79731	2.50971
3	0.6	1.34502	1.377062
3	0.8	1.33632	
3	1	1.25013	1.335962

Conclusion

This study extends the work of Pal and Mondal [23] to include the non-Newtonian fluid, modified viscous dissipation as well as equation of concentrate, heat generation, the equation of concentration with thermal diffusion and chemical reaction. The heat and mass transfer characteristics and MHD non-Darcy boundary-layer flow in an incompressible electrically flow over a linear shrinking sheet are studied by MATHEMATICAL. Highly non-linear of velocity, temperature and concentrate equations are converted into ODE by using suitable transformations. This system of equations is solved numerically by applying NDSolve command in MATHEMATICA package. The effects of Eckert number, Prandtl number, Hartmann number, local electric parameter, Schmidt number, and Soret number on temperature, velocity, and concentration are discussed through numerically and depicted graphically. The obtained results can be outlined as follows.

- By increasing Hartmann number the velocity increases while it decreases as E_1 increases.
- The temperature distribution increases with the increase of Eckert number, whereas it decreases as Prandtl number increases.
- The concentration increases with the decreases of both Schmidt and Soret numbers.

References

- [1] Pramanik, S., Casson Fluid Flow and Heat Transfer past an Exponentially Porous Stretching Sheet in Presence of Thermal Radiation, *Ain Shams Engineering Journal*, 5 (2014), 1, pp. 205-212
- [2] Ellahi, R., et al., Convective Radiative Plane Poiseuille Flow of Nanofluid through Porous Medium with Slip: An Application of Stefan Blowing, *Journal of Molecular Liquids*, 273 (2019), Jan., pp. 292-304
- [3] Akbar, N., Influence of Magnetic Field on Peristaltic Flow of a Casson Fluid in an a Symmetric Channel: Application in Crude Oil Refinement, *Journal of Magnetism and Magnetic Materials*, 378 (2015), Mar., pp. 463-468
- [4] Ellahi, R., et al., Mixed Convection Flow and Heat Transfer in Ferromagnetic Fluid over a Stretching Sheet with Partial Slip Effects, *Thermal Science*, 22 (2018), 6A, pp. 2515-2526
- [5] Hussanan, A., et al., Unsteady Boundary-layer Flow and Heat Transfer of a Casson Fluid past an Oscillating Vertical Plate with Newtonian Heating, *Plos One*, 9 (2014), 10, e108763
- [6] Abou-Zeid, M. Y., Effects of Thermal-Diffusion and Viscous Dissipation on Peristaltic Flow of Micropolar Non-Newtonian Nanofluid: Application of Homotopy Perturbation Method, *Results in Physics*, 6 (2016), Aug., pp. 481-495

- [7] El-Dabe, N. T., Abou-Zeid M. Y., The Wall Properties Effect Peristaltic Transport Micropolar Non-Newtonian Fluid with Heat and Mass Transfer, *Mathematical Problems in Engineering*, 2010 (2010), ID 898062
- [8] Hassan, M., et al., Convection Heat Transfer Flow of Nanofluid in a Porous Medium over Wavy Surface, *Physics Letters A*, 382 (2018), 38, pp. 2749-2753
- [9] Abou-Zeid, M. Y., Homotopy Perturbation Method for MHD Non-Newtonian Nanofluid Flow through a Porous Medium in Eccentric Annuli in Peristalsis, *Thermal Science*, 21 (2017), 5, pp. 2069-2080
- [10] El-Dabe, N. T., et al., Magnetohydrodynamic Peristaltic Flow of Jeffery Nanofluid with Heat Transfer through a Porous Medium in a Vertical Tube, *Applied Mathematics and Information Sciences*, 11 (2017), 4, pp. 1097-1103
- [11] Kataria, H. R., Patel, H. R., Heat and Mass Transfer in Magnetohydrodynamic (MHD) Casson Fluid Flow past over an Oscillating Vertical Plate Embedded in Porous Medium with Ramped Wall Temperature, *Propulsion and Power Research*, 7 (2018), 9, pp. 257-267
- [12] Shaaban, A. A., Abou-Zeid, M. Y., Effects of Heat and Mass Transfer on MHD Peristaltic Flow of a Non-Newtonian Fluid through a Porous Medium between Two Coaxial Cylinders, *Mathematical Problems in Engineering*, 2013 (2013), ID 819689
- [13] Ellahi, R., A Study on the Mixed Convection Boundary-layer Flow and Heat Transfer over a Vertical Slender Cylinder, *Thermal Science*, 18 (2014), 4, pp. 1247-1258
- [14] Raju, C. S. K., et al., Heat and Mass Transfer in Magnetohydrodynamic Casson Fluid over an Exponentially Permeable Stretching Surface, *Engineering Science and Technology, an International Journal*, 19 (2015), 1, pp. 45-52
- [15] Shehzad, S. A., et al., Effects of Mass Transfer on MHD Flow of Casson Fluid with Chemical Reaction and Suction, *Brazilian Journal of Chemical Engineering*, 30 (2013), 1, pp. 187-195
- [16] El-Dabe, N. T., et al., Magnetohydrodynamic Non-Newtonian Nanofluid Flow over a Stretching Sheet through a Non-Darcy Porous Medium with Radiation and Chemical Reaction, *Journal of Computational and Theoretical Nanoscience*, 12 (2015), 12, pp. 5363-5371
- [17] Alamri, S. Z., et al., Effects of Mass Transfer on MHD Second Grade Fluid towards Stretching Cylinder: A Novel Perspective of Cattaneo-Christov Heat Flux Model, *Physics Letters A*, 383 (2019), 2-3, pp. 276-281
- [18] Yousif, M. A., et al., Numerical Study of Momentum and Heat Transfer of MHD Carreau Nanofluid over Exponentially Stretched Plate with Internal Heat Source/Sink and Radiation, *Heat Transfer Research*, 50 (2019), 7, pp. 649-658
- [19] Hassan, M., et al., A Comparative Study of Magnetic and Non-Magnetic Particles in Nanofluid Propagating over a Wedge, *Canadian Journal of Physics*, 97 (2019), 3, pp. 277-285
- [20] Chirkov, V., et al., The Dependence of the Efficiency of Electrohydrodynamic Heat Exchanger on the Electric Conductivity of Liquid, *IEEE Transactions on Industry Applications*, 53 (2017), 3, pp. 2440-2445
- [21] Kuzko, A. E., Electrohydrodynamic Flows and Heat Transfer in the Blade-Plane Electrode System, *Fluid Dynamics*, 48 (2013), 3, pp. 310-320
- [22] Abou-Zeid, M. Y., Magnetohydrodynamic Boundary-Layer Heat Transfer to a Stretching Sheet Including Viscous Dissipation and Internal Heat Generation in a Porous Medium, *Journal of porous Media*, 14 (2011), 11, pp. 1007-1018
- [23] Pal, D., Mondal, H., Hydromagnetic Non-Darcy Flow and Heat Transfer over a Stretching Sheet in the Presence of Thermal Radiation and Ohmic Dissipation, *Communication in Nonlinear Science and Numerical Simulation*, 15 (2010), 5, pp. 1197-1209
- [24] Mohamed, M. A., Abou-Zeid, M. Y., MHD Peristaltic Flow of Micropolar Casson Nanofluid through a Porous Medium between Two Co-Axial Tubes, *Journal of Porous Media*, 22 (2019), 9, pp. 1079-1093
- [25] Abou-Zeid, M. Y., et al., Numerical Treatment and Global Error Estimation of Natural Convective Effects on Gliding Motion of Bacteria on a Power-Law Nanoslime through a Non-Darcy Porous Medium, *Journal of Porous Media*, 18 (2015), 11, pp. 1091-1106
- [26] Abou-Zeid, M. Y., Mohamed, M. A., Homotopy Perturbation Method for Creeping Flow of Non-Newtonian Power-Law Nanofluid in a Nonuniform Inclined Channel with Peristalsis, *Zeitschrift für Naturforschung – Section A Journal of Physical Sciences*, 72 (2017), 10a, pp. 899-907